A Methodological Framework for Parametric Combat Analysis

Maj. Dustin L. Hayhurst Sr.[a], John M. Colombi[b], Lt. Col. Robert A. Bettinger[c], David W. Meyer[d]

a USAF, Department of Systems Engineering and Management, Air Force Institute of Technology, 2950 Hobson Way, Wright-Patterson AFB, OH 45433

b Department of Systems Engineering and Management, Air Force Institute of Technology, 2950 Hobson Way, Wright-Patterson AFB, OH 45433

c USAF, Department of Aeronautics and Astronautics, Air Force Institute of Technology, 2950 Hobson Way, Wright-Patterson AFB, OH 45433

d Department of Aeronautics and Astronautics, Air Force Institute of Technology, 2950 Hobson Way, Wright-Patterson AFB, OH 45433

Abstract

This work proposes, explains, and demonstrates a methodological framework which affords decision-makers and policymakers the opportunity to accelerate the tempo and enhance the quality of the U.S. Department of Defense acquisitions community. The effective implementation of this framework will augment the warfighting capability of the U.S. Department of Defense against peer competitors and advance the security posture of the United States. This work provides a theoretical foundation for explaining the distribution of potential outcomes for certain types of warfare while contextualizing the research to the space domain. This framework utilizes reliability models to account for natural attrition while using combat models to account for induced attrition. The use of game-theoretic concepts enables the evaluation of heterogeneous force structures.

Keywords: combat modeling, game theory, space

Un marco metodológico para el análisis de combate paramétrico

Resumen

Este trabajo propone, explica y demuestra un marco metodológico que brinda a los responsables de la toma de decisiones y de políticas la oportunidad de acelerar el ritmo y mejorar la calidad de la comunidad de adquisiciones del Departamento de Defensa de EE. UU. La implementación efectiva de este marco aumentará la capacidad de guerra del Departamento de Defensa de los EE. UU.

doi: 10.18278/sesa.3.1.2

contra sus competidores y promoverá la postura de seguridad de los Estados Unidos. Este trabajo proporciona una base teórica para explicar la distribución de los posibles resultados de ciertos tipos de guerra al tiempo que contextualiza la investigación en el dominio espacial. Este marco utiliza modelos de confiabilidad para dar cuenta del desgaste natural mientras usa modelos de combate para dar cuenta del desgaste inducido. El uso de conceptos de teoría de juegos permite la evaluación de estructuras de fuerzas heterogéneas.

Palabras clave: modelado de combate, teoría de juegos, espacio

一项用于参数化作战分析的方法论框架

摘要

本研究提出、解释并证明了一个方法论框架，为决策者和政策制定者提供了加快美国国防部采购社区速度并提高其质量的机会。该框架的有效实施将增强美国国防部对抗同行竞争对手的作战能力，并提升美国的安全态势。本研究为解释某些战争类型的潜在结果分布提供了理论基础，同时将研究置于太空领域的情境中。该框架使用可靠性模型来解释自然减员，同时使用作战模型来解释诱发减员（induced attrition）。使用博弈论概念能评价异质的武装力量结构。

关键词：作战建模，博弈论，空间

Introduction and Background

Contextualization of Framework to the Space Domain

The universe holds countless numbers of galaxies including the Milky Way which holds countless numbers of stars, including Sol. The Sol System presents three regions known as the Inner Solar System, Outer Solar System, and Trans-Neptunian Region. The Inner Solar System encompasses the objects within the orbit of Jupiter. The Outer Solar System encompasses the objects between the orbits of Jupiter and Neptune, inclusive. The Trans-Neptunian Region extends from the orbit of Neptune to the boundary of the Sol System—considered either as the heliopause or the limit of space dominated by Sol's gravity. Together, the Inner Solar System and Outer Solar System constitute the Planetary Region—this work focuses primarily on the Planetary Region. The Trans-Neptunian Region holds the Kuiper Belt, Scattered Disc, heliopause, Detached Objects Region, and the theoretical Oort Cloud which may exist. Many objects move between multiple regions such as comets, which transit across most of the Solar System, and sednoids, which transit between the Scattered Disc and the Detached Objects Region. The Planetary Region encompasses 28 objects approximately rounded by the force of gravity including (listed by proximity to Sol and, in the case of natural satellites, proximity to planet) Sol, Mercury, Venus, Earth, Luna, Mars, Ceres, Jupiter, Io, Europa, Ganymede, Callisto, Saturn, Mimas, Enceladus, Tethys, Dione, Rhea, Titan, Iapetus, Uranus, Miranda, Ariel, Umbriel, Titania, Oberon, Neptune, and Triton. The Planetary Region also encompasses many non-spherical objects such as the asteroids of the Inner Solar System and the centaurs of the Outer Solar System. Any large-scale space conflict in the 10-to-20-year timeframe will likely be hosted by one of the 28 Planetary Region objects in approximate hydrostatic equilibrium. An evaluation of the habitability and resources of these celestial bodies, as well as the state and trajectory of human technology enables an educated prediction of humanity's exploration (conflict) path. This work predicts that humanity's exploration over the next 30 years will focus on Luna, Mars, Ceres, Callisto, and Titan. The Moon will probably undergo the most robust exploration and resource utilization and as such cislunar warfare constitutes the primary context for this work.

The Emerging Cislunar Domain

The Moon will likely transform into a vital economic hub for spacefaring nations. The focal points of this economic center will include resource harvesting, manufacturing, and lunar gateway transit. With respect to resource harvesting, the Moon may yield an abundant supply of rare-earth metals (REM) and Helium-3 (911Metallurgist, 2015). Even if humanity fails to profitably harvest resources directly from the Moon, Luna could host processing centers built to extract resources from asteroids. Japan already conducted successful sample returns from the asteroids Itokawa (Massachusetts Institute of Technology, 2016) and Ryugu (Shekhtman, 2020), while the United States currently attempts a successful sample return from the asteroid Bennu (Garner, 2021). Spacefaring nations may one day harvest precious and industrial metals from asteroids such as 16 Psyche, 1986 DA, and 2016 ED85 (Carter, 2021). In the development of the space economy, nations and organizations may determine that transporting asteroids or asteroid fragments to the Moon for extraction yields a greater profit than direct harvesting. Also, in consideration of an economic calculus, nations and organizations may decide to manufacture some items on the Moon rather than transport those items from Earth. The upcoming On-Orbit Servicing, Assembly, and Manufacturing 2 (OSAM-2, previously Archinaut One) mission scheduled to launch no earlier than 2022 will strive to mature the technology associated with microgravity manufacturing (Harbaugh, 2021). Finally, with humanity's desire to visit Mars and beyond, there exists a high probability that manufacturers will design some vehicles specialized for Earth-to-Moon transportation and others for transportation beyond the Moon. A lunar gateway would serve as a natural off-loading and on-loading point. The nation that controls Luna in part or in whole would reap tremendous economic benefits from these activities.

Evidence of Accelerating (Wartime) Space Capabilities

A key indicator of a nation's desire and ability to conduct a space conflict is the pace at which that nation develops space weapons and the demonstrable efficacy of those weapons. While the weaponization of space may take many forms, the fielding of effective direct ascent antisatellite (DA-ASAT) weapons provides an important benchmark for a nation's progress. Perhaps the five most pertinent events related to DA-ASAT weapons include:

> "the 1985 destruction of the US P78-1 Solwind satellite, using an air-launched ASM-135 (during the era of the Strategic Defense Initiative), the 2007 destruction of the Chinese FY-1C (Fengyun, "Wind and Cloud") satellite using a ground-launched SC-19, the 2008 destruction of the US USA-193 satellite using a sea-launched Standard Missile-3 (Operation Burnt Frost), … the 2019 destruction of the Indian Microsat-R satellite using a ground-launched Prithvi Defense Vehicle Mark-II (Mission Shakti, "Power")" (Hayhurst & Colombi, 2021), and the 2021 destruction of the Russian Kosmos 1408 using a ground-launched A-235 PL-19 Nudol (Wolfe, 2021).

During each test, the satellite was destroyed by its owner; the Russian and (especially) Chinese tests contributed significantly to the formation of geocentric Kessler fields.

The range of space weapon types extends beyond the kinetic DA-ASAT variants and can include dual-use technology. In 2010, China launched the SJ-12 (Shijian, "Practice") satellite into low Earth orbit (LEO) to conduct a series of rendezvous and proximity operations (RPO) maneuvers with SJ-06F; the two satellites likely made low-speed contact (Harrison, Johnson, & Roberts, 2018). In 2016, China launched the SJ-17 into geostationary orbit where it conducted proximity operations with multiple Chinese satellites (Roberts, 2021). The Chinese space endeavor made great strides during 2016, also launching the Aolong-1 ("Proud Dragon") and the Tianyuan-1 ("Fields and Gardens"). Aolong-1 matured robotic arm grappling technology, while Tianyuan-1 reportedly demonstrated spacecraft-to-spacecraft refueling. In 2021, China launched the SJ-21 into geostationary orbit where it docked with the defunct Beidou-2 ("Northern Dipper") G2 navigation satellite (Jones, 2022). In the beginning of 2022, SJ-21 pulled the defunct navigation satellite 3,000 km above the geostationary belt. While not a comprehensive review of space weaponry, these highlights provide insight into the steady transformation of space into a warfighting domain.

Another important indicator of a nation's space capabilities is the ability of that nation to visit celestial bodies. In a joint effort with the European Space Agency (ESA), Russia conducted a crash landing on Mars in 2016 with the ExoMars Schiaparelli EDM Lander—Russia intended to conduct a soft landing (NASA, n.d.). India conducted two hard landings on the Moon in 2008 and 2019. India planned for the impact probe released from the Chandrayaan-1 ("Moon Craft") to conduct a hard landing in 2008 (Barnett, n.d.). However, India intended the 2019 Chandrayaan-2 mission to conduct a soft landing (Williams, 2022). China conducted a Martian soft landing in 2021 with the Tianwen-1 ("Heavenly Questions") Lander (Stein, 2021). China also conducted multiple soft landings on the Moon's surface, the most impressive of which, Chang'e 5 ("Goddess of the Moon"), conducted a robotic sample return (The Planetary Society, n.d.). While China challenges the United States as the vanguard of space exploration, the U.S. free-market enterprise continues to experience tremendous and promising growth. Newcomers such as Virgin Galactic, Blue Origin, and especially SpaceX seek to challenge traditional mainstays such as the United Launch Alliance in the space industry sphere. In recent years, U.S. celestial surface exploration efforts focused primarily on Mars, with a series of successful soft landings on the Martian surface—the 2021 Perseverance mission constituting the most recent U.S. success (NASA, n.d.).

The Challenge of Keeping Pace in the U.S. DoD Acquisitions Community

In order for the United States to prevail against a peer competitor in a time of conflict, the U.S. Department of Defense (DoD) must develop an acquisitions community to field new capabilities within an operationally relevant timeframe. Pushing the current acquisitions community to achieve such a goal is a challenging, complex, and multifaceted undertaking which will not be comprehensively addressed within the scope of this article. This work will focus on a specific aspect of the endeavor to accelerate the acquisitions community: How does modeling and simulation inform the acquisitions organizations responsible for the procurement of DoD weapon systems? That is, which systems should the DoD develop and how many of those systems should the DoD produce? The aim of the methodological framework expounded in this paper is to enable the user to conduct parametric combat analysis to project the efficacy of various force compositions—such analysis should support the user in making intelligent and informed procurement decisions.

In order to effectively use the framework discussed in this article, the user must accept the premise that a knowledgeable person could capture the physical phenomena associated with various combat scenarios and express the dynamics of those scenarios in mathematical representations. The user must understand that these mathematical representations encompass parameters which the user may adjust to accurately represent a particular situation in an effort to make an educated prediction concerning the future. The user should not view parametric modeling as a replacement for agent-based modeling (e.g., Advanced Framework for Simulation, Integration, and Modeling) or high-fidelity physics-based modeling (e.g., Systems Tool Kit); parametric modeling is complementary to other modeling methods.

Article Outline

The literature review and mathematical introduction section of this paper will summarize similar research to provide context for this work and will provide the reader with an academic grounding for the material encompassed with the framework. The methodology section of this paper will present the framework, discuss how various phenomena influence a given instantiation of the framework, and provide an algorithm for a particular instantiation of the framework. The numerical demonstration of methodology section of this article will discuss the distribution of potential outcomes for different kinds of conflict and cover multiple notional scenarios between a blue force and a red force. Finally, the conclusion of this article will summarize this work and its recommendations.

Literature Review and Mathematical Introduction

This section reviews literature pertinent to this article, specifically focusing on probability theory, game theory, and combat modeling. This section provides a brief historical and contemporary account of parametric combat modeling while also reviewing the mathematical foundations of the framework.

Parametric Combat Modeling, Past and Present

Lanchester, the original intellectual luminary of parametric combat modeling, published his seminal work, *Aircraft in Warfare: The Dawn of the Fourth Arm*, in 1916. By the 1920s, Lotka and Volterra were researching biomathematics and theoretical ecology, independently developing models to characterize predator-prey interactions and interspecific competition. In 1959, Brackney introduced methods to connect parameter values directly to physical phenomena and encompass the fog of war within parametric modeling. These scholars used systems of differential equations which depended on homogenous force structures for effective implementation. In 1970, Bonder and Farrell attempted to alleviate this dependence on homogenous force structures; despite a commendable effort which made valuable contributions to the field, by their own admission they were not completely successful in closing the gap. The sphere of parametric combat modeling lacked an elegant approach for aggregating and characterizing the interactions of heterogeneous force structures. The following decades witnessed an explosion in computational abilities that led to the implementation of increasingly computationally intensive modeling efforts—while academics still studied the works of these luminaries, these methods became somewhat latent in the field of combat modeling (Hayhurst, Colombi, & Meyer, Aggregated space combat modeling, 2021).

The year 2021 witnessed the presentation of two independently developed strategies for addressing heterogeneous force structures in parametric combat modeling. Scardera and Cesul published their work on Media Interaction Warfare Theory (Scardera & Cesul, 2021), while Hayhurst et al. published their works fundamental to the integration of game-theoretic concepts (Hayhurst & Colombi, Game-Theoretic System Design in the Development of Space Power, 2021) into parametric combat models (Hayhurst, Colombi, & Meyer, Aggregated space combat modeling, 2021).

Probability Theory

The exponential distribution is a parametric distribution often used in reliability modeling to characterize the time to failure of entities within a data set. The probability density function (PDF) may be expressed as

$$f(t) = \frac{e^{-\frac{t}{\beta}}}{\beta}$$

with the support of ranging from zero to infinity and representing the scale parameter, which is also known as the characteristic lifespan; also exists as the expected value of the distribution (Casella & Berger, 2002). The exponential distribution is memoryless, tractable, and corresponds to the operational phase of life. The cumulative distribution function (CDF) may be presented as

$$F(t) = 1 - e^{-\frac{t}{\beta}}$$

The reliability function may be presented as

$$R(t) = e^{-\frac{t}{\beta}}$$

The hazard function may be presented as

$$h(t) = \frac{f(t)}{R(t)} = \frac{\frac{e^{-\frac{t}{\beta}}}{\beta}}{e^{-\frac{t}{\beta}}} = \frac{1}{\beta}$$

which corresponds to the constant failure rate of

$$\lambda = \frac{1}{\beta}$$

The Weibull distribution is a generalized form of the exponential distribution that can account for beneficial or deleterious aging at the cost of less tractability (Casella & Berger, 2002). The PDF of the Weibull distribution may be expressed as

$$f(t) = \frac{e^{-\frac{t^{\gamma}}{\beta}}}{\beta} \gamma t^{\gamma-1}$$

with the support of ranging from zero to infinity and representing the shape parameter of the distribution. indicates beneficial aging where failure rate decreases with respect to time; indicates memoryless aging (i.e., the exponential distribution); indicates deleterious aging where failure rate increases with respect to time; indicates the linear increase of failure rate with respect to time (i.e., the Rayleigh distribution). The CDF of the Weibull distribution may be presented as

$$F(t) = 1 - e^{-\frac{t^{\gamma}}{\beta}}$$

The reliability function may be presented as

$$R(t) = e^{-\frac{t^{\gamma}}{\beta}}$$

The hazard function may be presented as

$$h(t) = \frac{f(t)}{R(t)} = \frac{\frac{e^{-\frac{t^{\gamma}}{\beta}}}{\beta}\gamma t^{\gamma-1}}{e^{-\frac{t^{\gamma}}{\beta}}} = \frac{\gamma t^{\gamma-1}}{\beta}$$

The Weibull distribution is related to the exponential distribution through the random variable transformation

$$X_{Weibull} = X_{Exponential}^{\frac{1}{\gamma}}$$

Game Theory

Hayhurst and Colombi developed the Atomic Competitive Element (ACE) taxonomy for categorizing game-theoretic scenarios according to attributes desirable for the stability of an outcome within a game (Hayhurst & Colombi, Game-Theoretic System Design in the Development of Space Power, 2021). The ACE taxonomy uses red to designate balance optimality, yellow to designate Nash optimality, and blue to designate Pareto optimality; secondary colors are used to represent the combination of these attributes, white is used to represent the presence of all three attributes, and gray is used to represent the absence of all three attributes. Within a given cell of a normal-form game, red indicates the agents' payoffs are approximately the same, yellow indicates the cell is a pure strategy Nash equilibrium (no agent has incentive to unilaterally change their decision), and blue indicates the cell is on the Pareto front (no agent's payoff may be improved without diminishing another agent's payoff). Figure 1 is adapted from the work of Hayhurst and Colombi and presented to provide clarity on the ACE taxonomy.

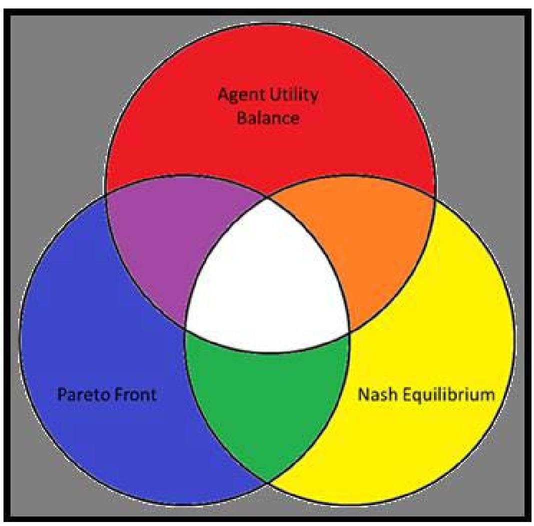

Figure 1. Atomic Competitive Element Taxonomy

Hayhurst and Colombi developed and presented eight specific ACEs for eight common games including Deadlock, Pure Coordination, Stag Hunt, Matching Pennies, Stoplight, Prisoner's Dilemma, Take or Share, and Chicken (Hayhurst & Colombi, 2021).

Combat Modeling Theory

The Lanchester Linear Law describes the attrition of two belligerents (described here as the blue force and red force or simply blue and red) under simplified engagement assumptions—two belligerents engage in a decisive conflict at a concrete focal point using unaimed fire; this law depends on the homogeneity of units on either side of the conflict and assumes a generally uniform distribution of fire from one side against the other. The Lanchester Linear Law may be presented as

$$\frac{dB}{dt} = -rRB$$

$$\frac{dR}{dt} = -bBR$$

such that

$$b \sim blue\ force\ attrition\ coefficient$$

$$r \sim red\ force\ attrition\ coefficient$$

$$B \sim size\ of\ the\ blue\ force$$

$$R \sim size\ of\ the\ red\ force$$

the case of the Lanchester Linear Law, the attrition rate for both blue and red is a function of the size of both forces. In this case, the fighting strength of each force may be presented as

$$F_B = bB$$

$$F_R = rR$$

The Lanchester Square Law assumes that each belligerent uses aimed fire and otherwise shares the same assumptions as the Lanchester Linear Law. The Lanchester Square Law may be presented as

$$\frac{dB}{dt} = -rR$$

$$\frac{dR}{dt} = -bB$$

Here, the blue (red) attrition rate is a function of the red's (blue's) force size. In this case, the fighting strength of each force may be presented as

$$F_B = bB^2$$

$$F_R = rR^2$$

For both the Lanchester Linear Law and the Lanchester Square Law, the force with the greater fighting strength will win the conflict (Lanchester, 1916).

The Bonder Law is a generalized form of the Lanchester Square Law and may be presented as

$$\frac{dB_m}{dt} = -\sum_{n=1}^{N} r_{m,n} R_n \quad for\ m = 1, 2, \dots, M$$

$$\frac{dR_n}{dt} = -\sum_{m=1}^{M} b_{m,n} B_m \quad for\ n = 1, 2, \dots, N$$

The Bonder Law shares the same assumptions as the Lanchester Square Law with the exception that the Bonder Law allows for heterogeneity within each belligerent force structure (Bonder & Farrell, 1970).

The Lotka-Volterra Interspecific Competition Law may be presented as

$$\frac{dN_1}{dt} = r_1 N_1 \left(\frac{K_1 - N_1 - \alpha N_2}{K_1}\right)$$

$$\frac{dN_2}{dt} = r_2 N_2 \left(\frac{K_2 - N_2 - \beta N_1}{K_2}\right)$$

such that

$r \sim respective\ per\ capita\ growth\ rate$

$N \sim respective\ population\ size$

$K \sim respective\ carrying\ capacity$

$\alpha \sim the\ per\ capita\ effect\ of\ entity\ 2\ on\ carrying\ capacity\ of\ entity\ 1$

$\beta \sim the\ per\ capita\ effect\ of\ entity\ 1\ on\ the\ carrying\ capacity\ of\ entity\ 2$

The Lotka-Volterra Interspecific Competition Law is based on the logistic growth model used to characterize intraspecific competition. The Lotka-Volterra Interspecific Competition Law assumes that two distinct, homogenous species compete over a common set of resources in a mutually deleterious manner to ensure population growth success up to the carrying capacity of the pertinent environment (Kingsland, 2015). In a conflict scenario in which the belligerents encompass certain characteristics of interspecific competition such as a carrying capacity, logistic growth, and competition over common resources, a Lanchester-Lotka-Volterra Hybrid Law (Hayhust, Colombi, & Meyer, 2021) may be presented as

$$\frac{dB}{dt} = B\left(\frac{K_B - B - rR}{K_B}\right)$$

$$\frac{dR}{dt} = R\left(\frac{K_R - R - bB}{K_R}\right)$$

where is still the respective carrying capacity of both entities, and have been replaced with the attrition rates of both entities, and and and are the force sizes. In this scenario, the goal of conflict is the establishment of a dominant ecological isocline. There exist four isocline scenarios which determine the fate of the conflict. In the case of a dominant blue isocline, the following inequalities hold:

$$K_B > \frac{K_R}{b}$$

$$\frac{K_B}{r} > K_R$$

The blue force will eliminate the red force and grow to its natural carrying capacity. Likewise, a dominant red isocline occurs when:

$$K_R > \frac{K_B}{r}$$

$$\frac{K_R}{b} > K_B$$

The red force will eliminate the blue force and grow to its natural carrying capacity. The isoclines present divergent bifurcation when:

$$K_B > \frac{K_R}{b}$$

$$K_R > \frac{K_B}{r}$$

In this scenario, the outcome of the conflict hinges on the parameter values of the respective carrying capacities and attrition coefficients as well as the initial size of each belligerent force. Finally, the isoclines present convergent behavior when:

$$\frac{K_B}{r} > K_R$$

$$\frac{K_R}{b} > K_B$$

In this case, the size of each force will converge to a steady equilibrium (Olson, 2014).

The Brackney Law may be presented as

$$\frac{dB}{dt} = -\frac{RBS_R}{T_B BS_R + V_B}$$

$$\frac{dR}{dt} = -\frac{BRS_B}{T_R RS_B + V_R}$$

such that

$S_B \sim$ *blue search rate, search volume per unit of time*

$V_B \sim$ *amount of volume the blue force may occupy*

$T_B \sim$ *amount of time required for red unit to destroy blue unit*

The Brackney Law integrates the fog of war into parametric modeling by describing two distinct, homogenous forces which must find the constituent parts of the adversary force before the destructive engagements may occur; this law assumes a random uniform distribution of each force throughout its respective volume (Brackney, 1959). The use of the Brackney Law requires knowledge of the specific, tangible capabilities of the fighting units which compose each force (Washburn & Kress, 2009). Hayhurst et al. adapted the Brackney Law for use in three-dimensional space (Hayhurst, Colombi, & Meyer, Aggregated space combat modeling, 2021).

Methodology

This section articulates the methodology of this work by describing the general mathematical construct of the integrated framework. This section also presents a mathematically symbolic demonstration of a specific instantiation of the framework to facilitate understanding.

General Mathematical Construct

Consider the integrated framework for analysis in its general form presented in Figure 2.

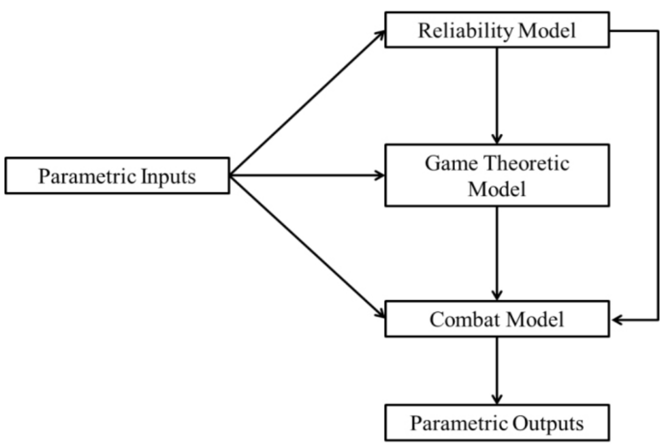

Figure 2. Integrated Framework in General Form

This integrated framework encompasses five modules which include the parametric inputs, reliability model, game-theoretic model, combat model, and parametric outputs. The necessary inputs and natural outputs of the framework are based on the specific models chosen by the user to fill in the reliability, game-theoretic, and combat modules; the user should choose models which accurately represent the physical phenomenon under consideration. This modularized approach provides flexibility and adaptability to the user.

The reliability model accounts for the "cold phase" of conflict—a long-duration, low-intensity period characterized by natural attrition (e.g., a spacecraft loses functionality because of battery decay). The reliability model uses a parametric distribution such as (but not limited to) the exponential or Weibull. The reliability model enables the framework to determine the losses associated with the cold phase of conflict for each belligerent. The reliability model receives information from the parametric inputs and provides information to the game-theoretic model and combat model.

The game-theoretic model is an strategic-normal form game which may manifest or resemble an atomic competitive element such as (but not limited to) Deadlock, Pure Coordination, Stag Hunt, Stoplight, Matching Pennies, Prisoner's Dilemma, Take or Share, or Chicken. The game-theoretic model enables the framework to calculate aggregate attrition coefficients from a larger set of pairwise attrition coefficients. The game-theoretic model receives information from the parametric inputs and reliability model and provides information to the combat model.

The combat model accounts for the "hot phase" of conflict—a short-duration, high-intensity period characterized by combat-induced attrition (e.g., a spacecraft loses functionality because of the hostile use of a directed energy weapon). The combat model uses a system of differential equations such as (but not limited to) the Lanchester Linear Law, Lanchester Square Law, Lotka-Volterra Equations, or Brackney Equations. The combat model enables the framework to determine the losses associated with the hot phase of conflict for each belligerent. The combat model receives information from the parametric inputs, reliability model, and game-theoretic model and provides information to the parametric outputs.

Specific Instantiation

This work will now transition from describing the general form of the framework to articulating a specific instantiation of the framework. The purpose of this illustration is to provide clarity on how the framework might be used; expounding the comprehensive set of uses for the framework in detail would be too expansive. During this symbolic demonstration, the quantity of a given fighting capability is expressed in a fictional currency for three reasons. First, using a fictional currency emphasizes the notional nature of this demonstration—a notional example facilitates public release and broad readership access. Second, while the combat models of this framework traditionally considered the number of fighting units within a capability such an approach might damage the composability of the model whenever a discrepancy in unit cost exists between capabilities. Accounting for the resources invested into a capability instead of the number of fighting units embodied within that capability helps to ensure composability within the framework. Finally, various real-world currencies differ in value and the purchasing power parity from one nation to the next might be starkly different. Essentially, the framework must capture how the purchasing power of a particular belligerent is spent—that is, any amount of purchasing power spent on a particular capability is assumed to be resources not spent on a separate, distinct capability within the same fighting force. The game-theoretic principles are then able to inform the effective allocation of finite resources.

With the groundwork for this example laid, consider two belligerents which act as peer competitors wherein each belligerent simultaneously invests a particular amount of currency into two capabilities each. As peer competitors, each belligerent must strive to match their strength to the weakness of their opponent over the course of combat. The game-theoretic model is, therefore, a two-by-two strategic-normal form matrix which embodies the Matching Pennies game. Consider that each capability is in the operational phase of its lifecycle. Therefore, the reliability model uses the exponential distribution. Consider that each capability does not reproduce, uses aimed fire at a decisive focal point of conflict, and is supported by an effective space domain awareness architecture. Therefore, the combat model uses the Lanchester Square Law. The correct module loadout of the general framework for this scenario is shown in Figure 3.

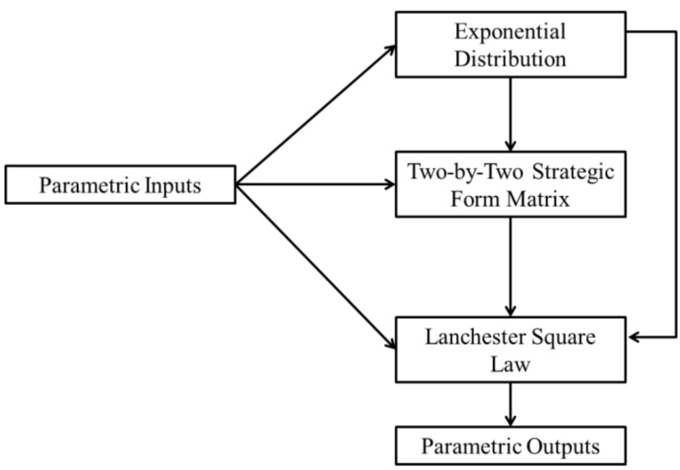

Figure 3. Framework with Module Loadout

Figure 4 provides a symbolic representation of Matching Pennies and affords clarity on the associated two-by-two strategic form matrix. Reference the appendix for a detailed walkthrough of the algorithm applicable to this specific instantiation.

Matching Pennies		Red Player	
		p_{R_1}	p_{R_2}
Blue Player	p_{B_1}	$b_{1,1}, r_{1,1}$	$b_{1,2}, r_{1,2}$
	p_{B_2}	$b_{2,1}, r_{2,1}$	$b_{2,2}, r_{2,2}$

Figure 4. Symbolic Representation of Matching Pennies

Numerical Demonstration of Methodology

This section provides a numerical demonstration of the methodological framework using the mathematical symbolic demonstration of the previous section as the foundational algorithm. The Python software package implemented in a Spyder integrated development environment (IDE) provides the computational capability for this demonstration; although a specific language and IDE are used for this demonstration, the methodological framework presented in this work is agnostic to any particular computational implementation. Any parameter values used in this demonstration are purely notional and only for the purpose of demonstrating the potential of the methodology of the previous section of this article. For simplicity and clarity, these scenarios assume each fighting unit of each capability consumes an equal amount of purchasing power; belligerents are not necessarily assumed to hold equal purchasing power.

Given parity, the distribution of outcomes for a Lanchester Square Law scenario under this framework follows a pronounced bimodality as shown in Figure 5. Values along the x-axis indicate the numerical discrepancy between the two belligerents at the end of the interaction while the y-axis values indicate the number of times such a discrepancy occurred. This divergence is caused by the bifurcating nature of the Lanchester Square Law which represents the underlying phenomena of aimed combat. That is, unless the dynamics of the conflict change or a latent advantage begins to manifest, small advantages will tend to snowball into increasingly larger advantages. This provides a theoretical foundation for explaining the extraordinary difficulty of predicting the outcome of a decisive peer conflict using aimed fire; approximately mean outcomes of such a conflict are extremely unlikely to occur. Attrition coefficients assume an expected value and variability of one. In the space context, these potential outcomes are associated with a high domain awareness constrained conflict using cryptographic, cyber, directed energy, and robotic weapons supported by a robust space domain awareness architecture.

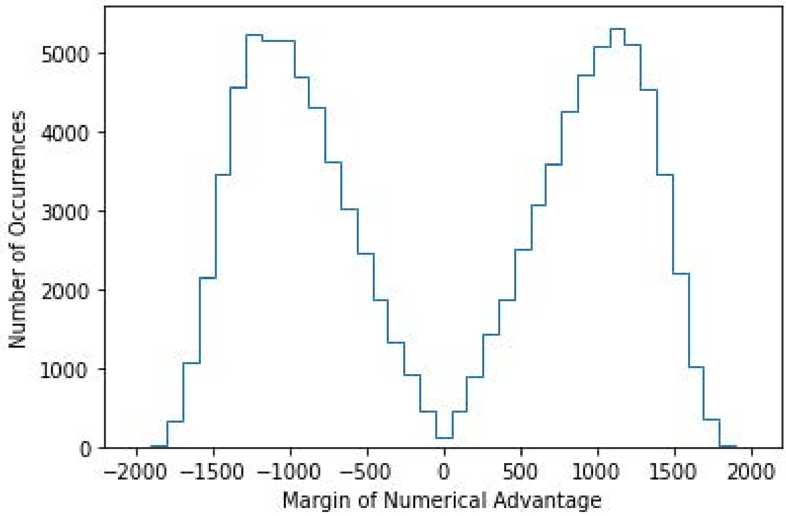

Figure 5. Bimodal Lanchester Square Law Outcome Distribution – 100,000 Runs

Given parity, the distribution of outcomes for a Lanchester Linear Law scenario under this framework presents a trapezoidal shape as shown in Figure 6. Unaimed combat does not experience the snowball effect of aimed combat; outcomes within a range of numerical parity are approximately equally likely. Attrition coefficients assume an expected value and variability of one. In the space context, these potential outcomes are associated with unconstrained conflict which uses the capabilities of constrained conflict in addition to electromagnetic, nuclear, radioactive, kinetic (which generate Kessler fields), and chemical weapons.

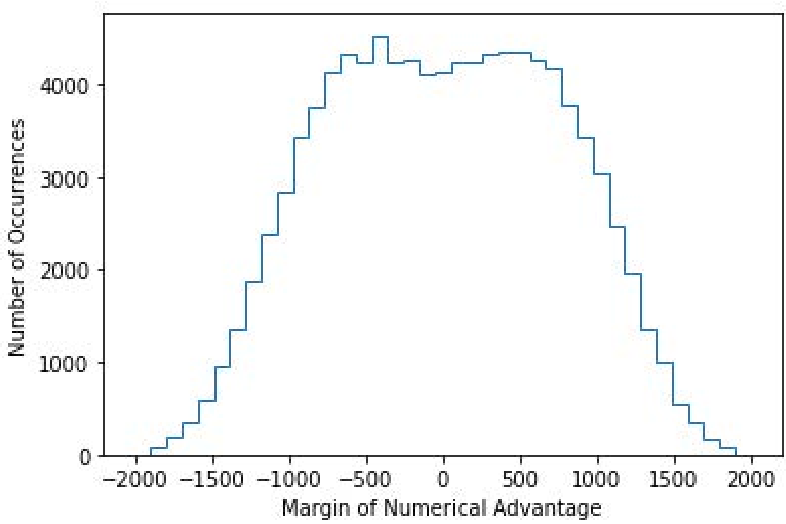

Figure 6. Trapezoidal Linear Law Outcome Distribution – 100,000 Runs

Given parity, the distribution of outcomes for a Brackney Law scenario under this framework presents a shape in between the square and linear law distribution shapes as shown in Figure 7. This result is expected as the Brackney Law behavior shifts from linear law behavior to square law behavior as the conflict phases from kill-time dominated to search-time dominated. Attrition coefficients assume an expected value and variability of one. In the space context, these potential outcomes are associated with low domain awareness constrained conflict which uses the same capabilities of high domain awareness constrained conflict unsupported by a robust space domain awareness architecture.

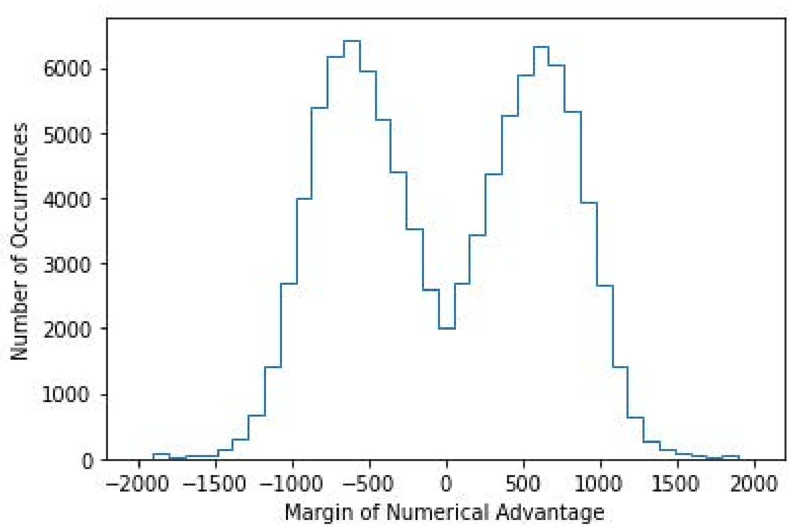

Figure 7. Brackney Law Outcome Distribution – 100,000 Runs

Given parity, the distribution of outcomes for a Hybrid Law scenario under this framework presents a uniform shape with two spikes at the extremes as shown in Figure 8. The uniform component of the distribution represents stable equilibria while the spikes represent extinction events. Attrition coefficients assume an expected value and variability of one while carrying capacities assume a value of 2,000. In the space context, these potential outcomes are associated with economic conflict wherein spacecraft manufacture spacecraft and nations attempt to monopolize the harvest space resources through aggressive economies of scale and learning curve efficiencies.

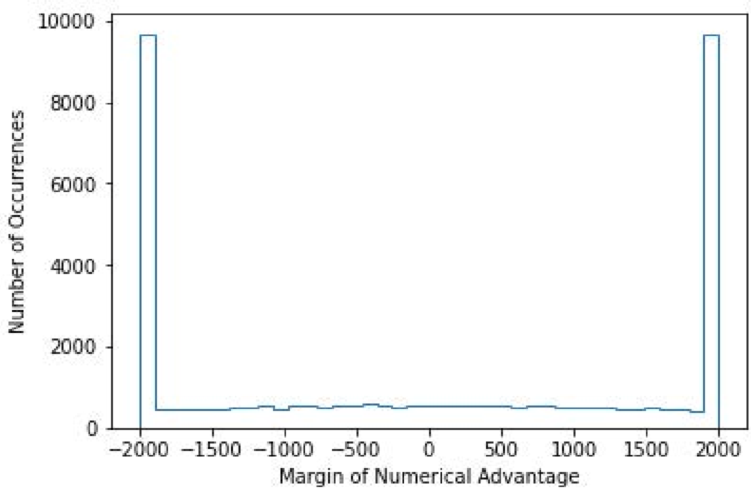

Figure 8. Hybrid Law Outcome Distribution – 100,000 Runs

Figures 9 through 11 and 13 afford further understanding of how parity shapes outcome distributions—each figure displays the results of a Lanchester Square Law conflict over 10,000 simulation runs in which positive numerical values along the x-axis indicate a blue numerical advantage at the end of the conflict while negative values indicate a red numerical advantage. Contextualized to the space domain, each set of potential outcomes is associated with high domain awareness constrained conflict. The difference in distributions arises from adjusting the amounts and pairwise efficacies of two hypothetical capabilities (directed energy and robotic weapons) of two belligerents. Figure 9 demonstrates the case of qualitative and quantitative parity. Attrition coefficients assume an expected value and variability of one.

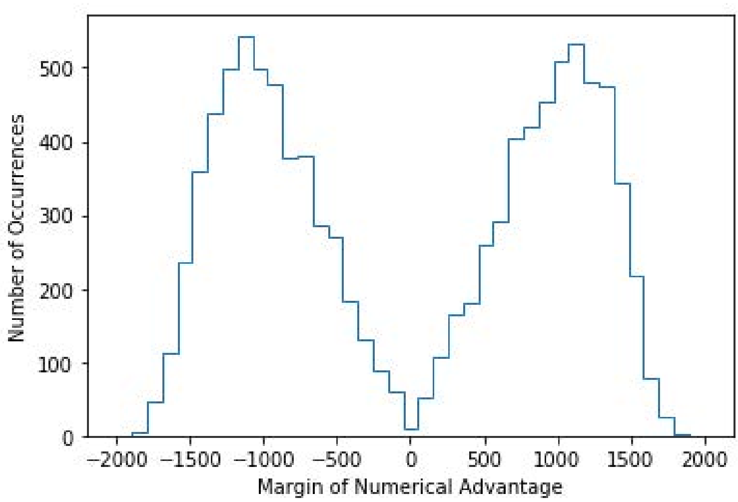

Figure 9. Balanced Parity

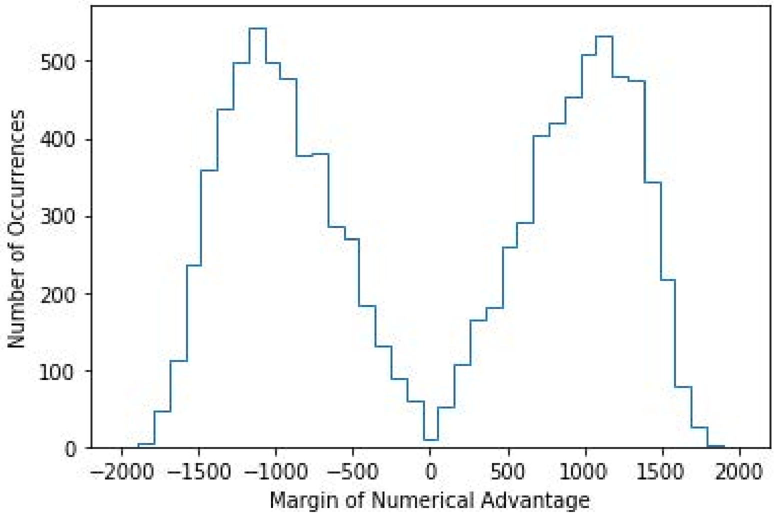

Figure 9. Balanced Parity

Figure 10 illustrates the case wherein the expected quality of blue forces is four times greater than that of red forces but red presents a force which is quantitatively twice as large as blue forces. Blue boasts 500 fighting units of each capability while red boasts 1,000 fighting units of each capability. All red specific attrition coefficients assume an expected value of one while blue attrition coefficients assume an expected value of four; the variability of all attrition coefficients is one.

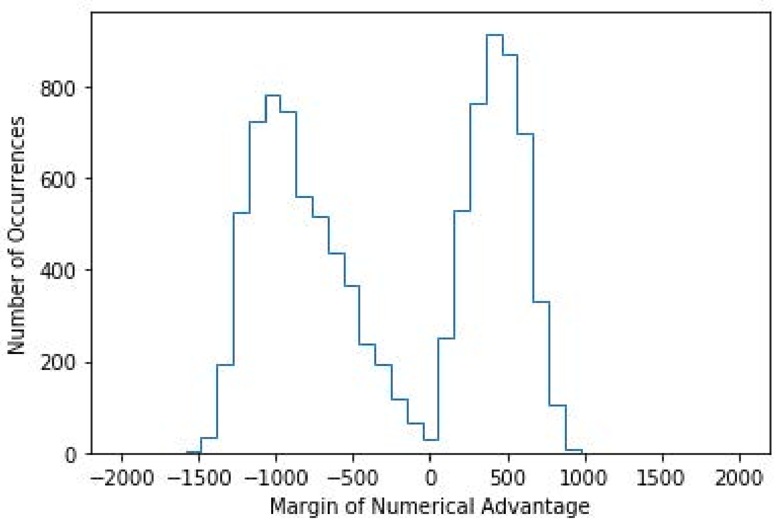

Figure 10. Imbalanced Parity

Figure 11 illustrates the case wherein red is provided with a ten percent boost to the quantity and quality of its forces relative to blue; conferring such an advantage significantly impacts the distribution of potential conflict outcomes. Blue boasts 500 units of each capability with expected attrition coefficients of one. Red boasts 550 units of each capability with expected attrition coefficients of 1.10.

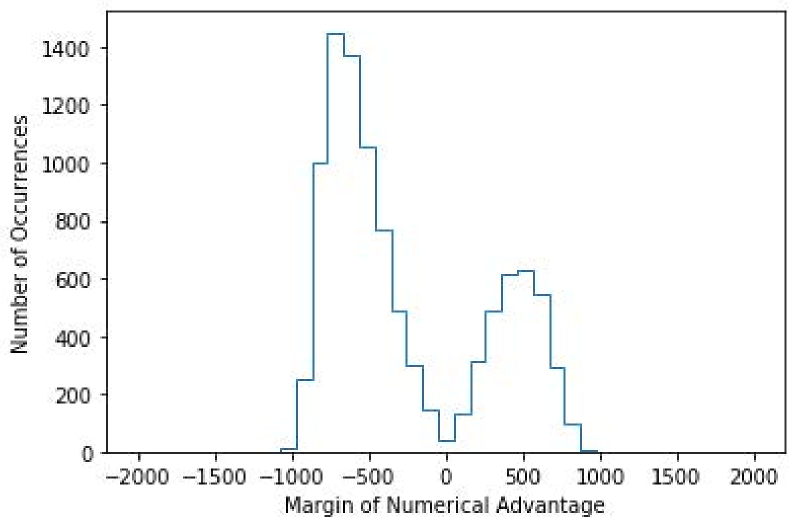

Figure 11. Lack of Parity

While Figure 11 illustrates a straightforward way for a belligerent to gain a numerical advantage in conflict, more nuanced methods do exist. Consider a space conflict scenario between blue and red using directed energy weapons (DEW) and robotic weapons (RW) in which blue fields capabilities with expected pairwise attrition coefficients of one, two, three, and four, while red fields capabilities with coefficients four, three, two, and one as shown in Figure 12. Consider that blue and red present the same number of total fighting units.

Cislunar Conflict		Red	
		DEW	RW
Blue	DEW	1, 4	2, 3
	RW	3, 2	4, 1

Figure 12. Cislunar Conflict Game

In such a case, blue DEW perform poorly against red DEW and marginally against red RW; blue RW perform well against red DEW and dominantly against red RW. While such a scenario may seem completely balanced, blue holds an incredibly advantageous position through game-theoretic system design since blue RW versus red DEW exists as a pure strategy Nash equilibrium. However, even in such an advantageous position, blue must still present sufficient competence in force composition to finish the conflict in a numerically advantageous position. For example, if blue invests in 1,500 DEW and 500 RW while red invests in 500 DEW and 1,500 RW, red will likely end the conflict in a numerically advantageous position, as shown in Figure 13.

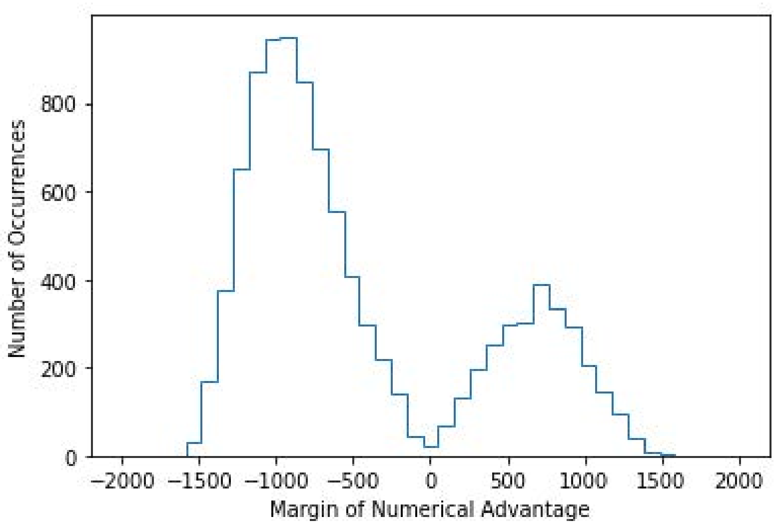

Figure 13. Resource Parity, Suboptimal Blue Force Composition

A competent opponent will take advantage of unforced game-theoretic errors.

Conclusion

This work presented a methodological framework for parametric combat analysis in order to improve the security posture of the United States. After discussing pertinent literature and the methodological framework as well as contextualizing this work to the space domain, this article provided demonstrations of the framework. Though contextualized in this work to the space domain where necessary, this methodological framework could be applied to any domain of combat given that the user characterizes the underlying phenomena with the correct mathematical representations.

The author recommends the U.S. DoD acquisitions community uses this methodological framework to accelerate the capability development tempo to an operationally relevant timeframe. The flexible modularity of this framework enhances the ability of the user to customize the modeling and simulation as necessary. The framework is compatible with game-theoretic concepts which can help the user to optimize force compositions and predict agent behavior. While not a wargame in and of itself, this framework could be used as a wargaming tool to bolster objective analysis. The United States faces multiple peer competitors and is steadily losing military preeminence. Spending significant resources on national defense is no longer sufficient; the United States must invest in capabilities wisely to effectively compete in an increasingly multipolar world.

References

911Metallurgist. (2015, May 29). *The Lunar Gold Rush: How Moon Mining Could Work*. Retrieved from NASA Jet Propulsion Laboratory: https://www.jpl.nasa.gov/infographics/the-lunar-gold-rush-how-moon-mining-could-work

Barnett, A. (n.d.). *Chandrayaan-1 / Moon Impact Probe*. Retrieved from Solar System Exploration: https://solarsystem.nasa.gov/missions/chandrayaan-1/in-depth/

Bonder, S., & Farrell, R. (1970). *Development of Models for Defense Systems Planning.* Ann Arbor : The University of Michigan.

Brackney, H. (1959). The Dynamics of Military Combat. *Operations Research*, 30-44.

Carter, J. (2021, October 19). *Space Mining: Scientists Discover Two Asteroids Whose Precious Metals Would Exceed Global Reserves*. Retrieved from Forbes: https://www.forbes.com/sites/jamiecartereurope/2021/10/19/the-age-of-space-mining-just-got-closer-as-scientists-discover-two-asteroids-whose-precious-metals-would-exceed-global-reserves/?sh=2c6aee3e713b

Casella, G., & Berger, R. L. (2002). *Statistical Inference: Second Edition.* Belmont: Brooks/Cole Cengage Learning.

Garner, R. (2021, April 14). *OSIRIS-REx.* Retrieved from NASA: https://www.nasa.gov/osiris-rex

Harbaugh, J. (2021, March 5). *STMD: Tech Demo Missions*. Retrieved from NASA: https://www.nasa.gov/mission_pages/tdm/osam-2.html

Harrison, T., Johnson, K., & Roberts, T. (2018). *Space Threat Assessment 2018.* Washington D.C.: CSIS.

Hayhurst, D., & Colombi, J. (2021). Game-Theoretic System Design in the Development of Space Power. *Air & Space Power Journal.*

Hayhurst, D., Colombi, J., & Meyer, D. (2021). Aggregated space combat modeling. *Journal of Defense Modeling and Simulation*.

Jones, A. (2022, January 27). *China's Shijian-21 towed dead satellite to a high graveyard orbit*. Retrieved from Space News: https://spacenews.com/chinas-shijian-21-spacecraft-docked-with-and-towed-a-dead-satellite/

Kingsland, S. (2015). Alfred J. Lotka and the origins of theoretical population ecology. *Proceedings of the National Academy of Sciences of the United States of America*.

Lanchester, F. (1916). *Aircraft in Warfare: The Dawn of the Fourth Arm.* London: Constable and Company Limited.

Massachusetts Institute of Technology. (2016). *Asteroid Mining*. Retrieved from The Future of Strategic Natural Resources: https://web.mit.edu/12.000/www/m2016/finalwebsite/solutions/asteroids.html

NASA. (n.d.). *ExoMars 2016 Mission (ESA/Roscosmos)*. Retrieved from Mars Exploration Program: https://mars.nasa.gov/mars-exploration/missions/esa-exomars-2016-tgo/

NASA. (n.d.). *Mars 2020 Mission Perseverence Rover*. Retrieved from NASA Science: https://mars.nasa.gov/mars2020/

Olson, J. (2014, October 8). *Modelling Interspecific Competition*. Retrieved December 20, 2020, from YouTube: https://www.youtube.com/watch?v=obasfCufOr0

Roberts, T. (2021, March 31). *Unusual Behavior in GEO: SJ-17*. Retrieved from Aerospace Security: https://aerospace.csis.org/data/unusual-behavior-in-geo-sj-17/

Scardera, M. P., & Cesul, B. T. (2021). Media Interaction Warfare Theory: A Novel Analytic Process Supporting Space Warfare Planning Operations. *Air & Space Power Journal*, 37-59.

Shekhtman, L. (2020, December 7). *Asteroid Ryugu Dust Delivered to Earth; NASA Astrobiologists Prepare to Probe It*. Retrieved from NASA: https://www.nasa.gov/feature/goddard/2020/asteroid-ryugu-dust-delivered-to-earth-nasa-astrobiologists-prepare-to-probe-it

Stein, V. (2021, February 8). *Tianwen-1: China's first Mars mission*. Retrieved from

Space.com: https://www.space.com/tianwen-1.html

The Planetary Society. (n.d.). *Chang'e-5: China's Moon sample return mission*. Retrieved from The Planetary Society: https://www.planetary.org/space-missions/change-5

Washburn, A., & Kress, M. (2009). *Combat Modeling.* New York: Springer.

Williams, D. (2022, January 7). *NASA Space Science Data Coordinated Archive*. Retrieved from NASA: https://nssdc.gsfc.nasa.gov/nmc/spacecraft/display.action?id=2019-042A

Wolfe, F. (2021, November 15). *Russian Direct Ascent ASAT Test Generates More Than 1,500 Pieces of Trackable Debris*. Retrieved from Defense Daily: https://www.defensedaily.com/russian-direct-ascent-asat-test-generates-more-than-1500-pieces-of-trackable-debris/space/

Appendix

In order to carry out the analysis of this scenario using the integrated framework, utilize the following process. First, the user supplies 26 parametric inputs including the initial investment in each capability ($B_{1\alpha}$, $B_{2\alpha}$, $R_{1\alpha}$, $R_{2\alpha}$), the characteristic lifespan for the units of currency for each capability ($\beta_{B_{1\alpha}}$, $\beta_{B_{2\alpha}}$, $\beta_{R_{1\alpha}}$, $\beta_{R_{2\alpha}}$), the expected value and variability associated with each pairwise attrition coefficient ($\mu_{b_{1,1}}$, $\mu_{b_{1,2}}$, $\mu_{b_{2,1}}$, $\mu_{b_{2,2}}$, $\mu_{r_{1,1}}$, $\mu_{r_{1,2}}$, $\mu_{r_{2,1}}$, $\mu_{r_{2,2}}$, $[\sigma^2]_{b_{1,1}}$, $[\sigma^2]_{b_{1,2}}$, $[\sigma^2]_{b_{2,1}}$, $[\sigma^2]_{b_{2,2}}$, $[\sigma^2]_{r_{1,1}}$, $[\sigma^2]_{r_{1,2}}$, $[\sigma^2]_{r_{2,1}}$, $[\sigma^2]_{r_{2,2}}$), and the time spent in the cold and hot phases of the conflict (t_c, t_h). Next, generate a normal distribution for each pairwise attrition coefficient and randomly draw a number from each of those normal distributions to determine the value for each pairwise attrition coefficient.

$$f(b_{1,1}) = \frac{1}{\sqrt{2\pi[\sigma^2]_{b_{1,1}}}} e^{-\frac{\left(b_{1,1}-\mu_{b_{1,1}}\right)^2}{2[\sigma^2]_{b_{1,1}}}}$$

$$\dots$$

$$f(r_{2,2}) = \frac{1}{\sqrt{2\pi[\sigma^2]_{r_{2,2}}}} e^{-\frac{\left(r_{2,2}-\mu_{r_{2,2}}\right)^2}{2[\sigma^2]_{r_{2,2}}}}$$

Calculate the remaining investment after natural attrition during the cold phase by multiplying the initial investment by the exponential reliability function.

$$B_1 = B_{1\alpha} e^{-\frac{t_c}{\beta_{B_{1\alpha}}}}$$

$$B_2 = B_{2\alpha} e^{-\frac{t_c}{\beta_{B_{2\alpha}}}}$$

$$R_1 = R_{1\alpha} e^{-\frac{t_c}{\beta_{R_{1\alpha}}}}$$

$$R_2 = R_{2\alpha} e^{-\frac{t_c}{\beta_{R_{2\alpha}}}}$$

Calculate the game-theoretic mixed strategy as a population parameter for each belligerent. To do this, calculate the proportion of the remaining investment which each capability constitutes. In this game-theoretic context, the mixed strategy exists as a population parameter wherein instead of two decisions being made with certain probabilities there exist two populations with certain proportions of subpopulations.

$$p_{B_1} = \frac{B_1}{B_1 + B_2}$$

$$p_{B_2} = \frac{B_2}{B_1 + B_2}$$

$$p_{R_1} = \frac{R_1}{R_1 + R_2}$$

$$p_{R_2} = \frac{R_2}{R_1 + R_2}$$

Determine the aggregate attrition coefficients by multiplying the probabilities within the three-dimensional probability mass function by the associated payoffs. The payoffs are the pairwise attrition coefficients.

$$b = p_{B_1}p_{R_1}b_{1,1} + p_{B_1}p_{R_2}b_{1,2} + p_{B_2}p_{R_1}b_{2,1} + p_{B_2}p_{R_2}b_{2,2}$$
$$r = p_{B_1}p_{R_1}r_{1,1} + p_{B_1}p_{R_2}r_{1,2} + p_{B_2}p_{R_1}r_{2,1} + p_{B_2}p_{R_2}r_{2,2}$$

Calculate the aggregate remaining investment for each belligerent after natural attrition.

$$B = B_1 + B_2$$
$$R = R_1 + R_2$$

Enable the simulation to run for the hot phase time using the Lanchester Square Law system of differential equations.

$$\frac{dB}{dt} = -rR$$
$$\frac{dR}{dt} = -bB$$

Calculate the margin of victory (or defeat) at the end of the conflict.

$$\mathrm{M} = B|_{t=t_h} - R|_{t=t_h}$$

Since the simulation is stochastic, the user should run the simulation over multiple iterations—such an approach will provide a range of outcomes to articulate the possible results of the physical phenomena.